MOX-Report No. 44/2018

Modelling spatially dependent functional data by spatial regression with differential regularization

Bernardi, M.S.; Sangalli, L.M.

MOX, Dipartimento di Matematica
Politecnico di Milano, Via Bonardi 9 - 20133 Milano (Italy)

mox-dmat@polimi.it http://mox.polimi.it

Modelling spatially dependent functional data by spatial regression with differential regularization

Mara S. Bernardi[1] Laura M. Sangalli[1*]

[1] MOX - Department of Mathematics, Politecnico di Milano, Milano, Italy

1 Introduction

In this chapter we describe the modelling of spatially dependent functional data by regression with differential regularization [23]. The chapter is based on [3].

Spatial regression with differential regularization defines the unknown spatial field f as deterministic, and models the spatial (or spatio-temporal) variation of the phenomenon under study via a regularizing term involving a Partial Differential Equation (PDE). This contrasts with the main approach followed in the other chapters of the book, where the unknown field is modeled as stochastic and the spatial variation of the phenomenon is controlled via the definition of the covariance structure of the random field.

The different modelling of the spatial variation considered by spatial regression with differential regularization, combined with the use of advanced numerical analysis techniques, such as finite element methods and isogeometric analysis based on splines and extensions, leads to important advantages. One main advantage, that we here illustrate, is the ability to efficiently deal with data distributed over a spatial domain featuring peninsulas, islands, holes and other complex geometries that influence the phenomenon under study. Moreover, the method can comply with specific conditions at the boundaries of the problem domain, which is fundamental in many applications to obtain meaningful estimates.

As an illustrative example, consider the estimation of the temporal evolution of the amount of per capita municipal waste produced in the towns of Venice province. Figure 1 shows the Venice province, with dots indicating town centers, including municipalities and other tourist localities of particular relevance. The province boundary is shown by a line, highlighting the irregular shape of the province administrative borders and its complex coastlines, with the Venice lagoon partly enclosed by elongated peninsulas and small islands.

*Corresponding author. E-mail: laura.sangalli@polimi.it

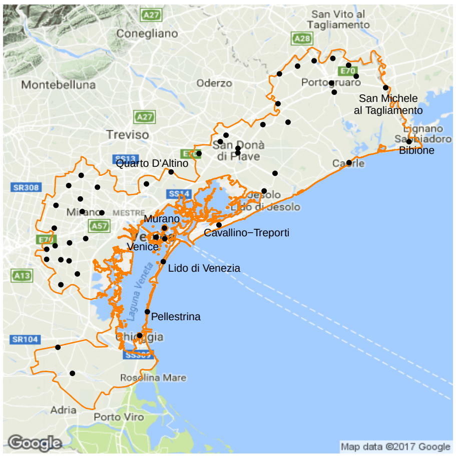

Figure 1: Spatial domain of the Venice waste data, with a line highlighting the province boundary and dots indicating the towns centers. Figure adapted from [3].

The data are measurements from 1997 to 2011 of the yearly amount of per capita municipal waste (total kg divided by the number of municipality residents) and are provided by the Arpav, the Agenzia regionale per la prevenzione e protezione ambientale del Veneto. Figure 2 shows the temporal evolution of the production of per capita waste in the towns of Venice province; Figure 3 is a bubble plot of the data at a fixed year, 2006. The phenomenon portrayed by these data is expressed differently in different parts of the domain. Consider for instance the two towns of Cavallino-Treporti (in the peninsula at the north-east of Venice) and Quarto d'Altino (north of Venice), indicated by black dots in Figure 3. The temporal evolution of the production of per capita municipal waste in the two towns, highlighted in Figure 2, is rather different, with strongly increasing and high values in the seaside and tourist town of Cavallino-Treporti, opposed to the not increasing and lower values measured in the hinterland town of Quarto d'Altino. These two towns are close in terms of their geodesic distance, but they are much further apart in terms of land connections, as they are separated by the Venice lagoon. Appropriately accounting for the shape of the domain, characterized by the strong concavity formed by the lagoon, is crucial to accurately handle these data.

When analyzing the temporal evolutions of the amount of per capita municipal waste, we shall make a strong simplification of the nature of these data, and consider them in the framework of geostatistical functional data [8], where the datum is observable in principle in any point of the domain, instead of in the framework of functional areal data. As detailed in Paragraph 4, this is due to the fact that we miss the information concerning the urbanized areas of the municipalities, where the type of waste here considered (that does not include agricultural, industrial, construction/demolition and hazardous waste) is produced.

This book reviews in detail many of recently proposed methods for the analysis of spatially dependent functional data, mostly in the framework of kriging for functional data [see, e.g, 11, 8, 18, 10, 5, 16, 17, 12]. On the other hand, these methods, as well as the extensive literature in the more classical spatial-time data framework [see, e.g., 6, and references therein], are not well suited to handle data distributed over irregular domains, as they do not take into account the shape of the domain; they would for instance smooth across concave boundary regions, thus closely linking data points that are in fact far apart by land connections.

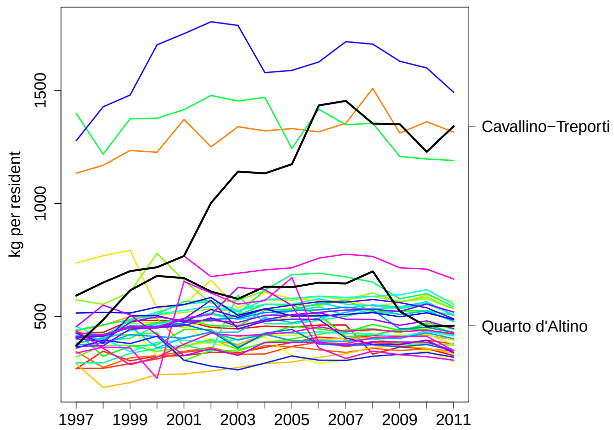

Figure 2: Temporal evolution of the yearly per capita production (kg per resident) of municipal waste in the towns of Venice province. Figure adapted from [3].

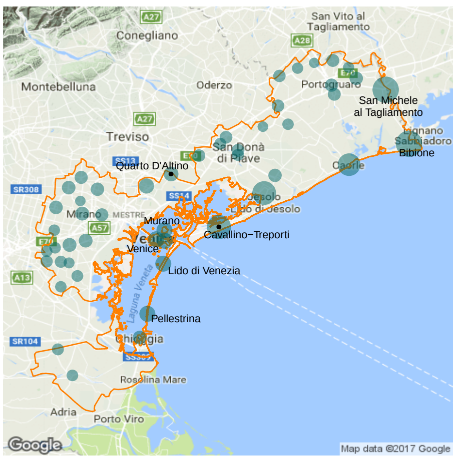

Figure 3: Per capita production (kg per resident) of municipal waste in the towns of Venice province in 2006. The data include all municipalities of Venice province and additional four localities (Bibione, Murano, Lido di Venezia and Pellestrina), that do not constitute a municipality on their own, but have been included due to their tourist relevance and their location on the domain. For these additional four localities, the considered datum is a replicate of the datum of their corresponding municipalities (see Paragraph 4). Figure adapted from [3].

Recent methods for the analysis of spatio-temporal data that instead specifically account for the geometry of the domain of interest are described in [1] and [15]. These models are based on the spatial smoother proposed by [26]. Here, we describe the method proposed in [3], that extends the spatial regression models with differential regularization described in [22], [23] and [2]. The model is implemented in R [20], based on the package fdaPDE [14].

2 Spatial regression with differential regularization for geostatistical functional data

Let $\Omega \subset \mathbb{R}^2$ be a bounded spatial domain, possibly with an irregular geometry, and let $\{\mathbf{p}_i = (x_i, y_i) \in \Omega; i = 1, ..., n\}$ be a set of n spatial locations within this domain. Moreover, consider m time instants $\{t_j \in T; j = 1, ..., m\}$ over the temporal interval $T = [t_{start}, t_{end}] \subset \mathbb{R}$. Let z_{ij} be the value of a real-valued variable observed at location $\mathbf{p}_i$ and time instant t_j. Additionally, let $\mathbf{w}_{ij} \in \mathbb{R}^q$ be a vector of q space-time varying covariates associated with the observation z_{ij} at the spatio-temporal locatio $(\mathbf{p}_i, t_j)$. In our illustrative application, the spatial domain Ω is the province of Venice, the spatial locations $\mathbf{p}_i$ are the centers of the towns, the time instants t_j are the years between 1997 and 2011, the variable of interest z_{ij} is the amount of per capita municipal waste produced in the town i and year t_j; furthermore, since intuition suggest that the tourism may play an important role in the production of waste, we consider as covariate w_{ij} the number of beds in accommodation facilities in the town i and year t_j.

Assume the following semi-parametric generalized additive model

$$z_{ij} = \mathbf{w}_{ij}^T \boldsymbol{\beta} \, + \, f(\mathbf{p}_i, t_j) \, + \, \varepsilon_{ij} \quad i = 1, ..., n, \;\; j = 1, ..., m, \tag{1}$$

where $\boldsymbol{\beta} \in \mathbb{R}^q$ is a vector of q regression coefficients, $f(\mathbf{p}, t) : \Omega \times T \to \mathbb{R}$ is an unknown smooth spatio-temporal function, and $\{\varepsilon_{ij}; i = 1, ..., n; j = 1, ...m\}$ are independently distributed residuals with mean zero and constant variance σ^2. As detailed in Paragraph 2.4, one may as well consider a model without covariates. In this case the values z_{ij} can be directly seen as discrete and noisy observations of dependent functional data, either spatially dependent curves or time dependent surfaces.

The vector of regression coefficients $\boldsymbol{\beta}$ and the spatio-temporal field f can be jointly estimated minimizing a penalized sum of square error functional. In particular, in [3] we propose to consider two roughness penalties that account separately for the regularity of the field in space and in time. Let

$$\begin{aligned} J(f, \boldsymbol{\beta}) = & \sum_{i=1}^{n} \sum_{j=1}^{m} \big(z_{ij} - \mathbf{w}_{ij}^T \boldsymbol{\beta} - f(\mathbf{p}_i, t_j) \big)^2 \\ & + \lambda_\Omega \int_T \int_\Omega \Big(\Delta f(\mathbf{p}, t) \Big)^2 d\mathbf{p} dt \, + \, \lambda_T \int_\Omega \int_T \Big(\frac{\partial^2 f(\mathbf{p}, t)}{\partial t^2} \Big)^2 dt d\mathbf{p}, \end{aligned} \tag{2}$$

where the two smoothing parameters $\lambda_\Omega > 0$ and $\lambda_T > 0$ weight the penalizations respectively in space and time; the choice of these parameters will be discussed in Paragraph 2.3. The partial differential operator $\Delta f(\mathbf{p}, t) = \frac{\partial^2 f}{\partial x^2}(\mathbf{p}, t) + \frac{\partial^2 f}{\partial y^2}(\mathbf{p}, t)$ is the Laplacian of the spatial component of the field; it provides the local curvature of the spatial field, at a given time t. The Laplacian is invariant to rigid transformations of the spatial coordinates, thus ensuring that the concept of smoothness does not depend on the arbitrary choice of the coordinate system. The smoothness penalties in (2) are isotropic

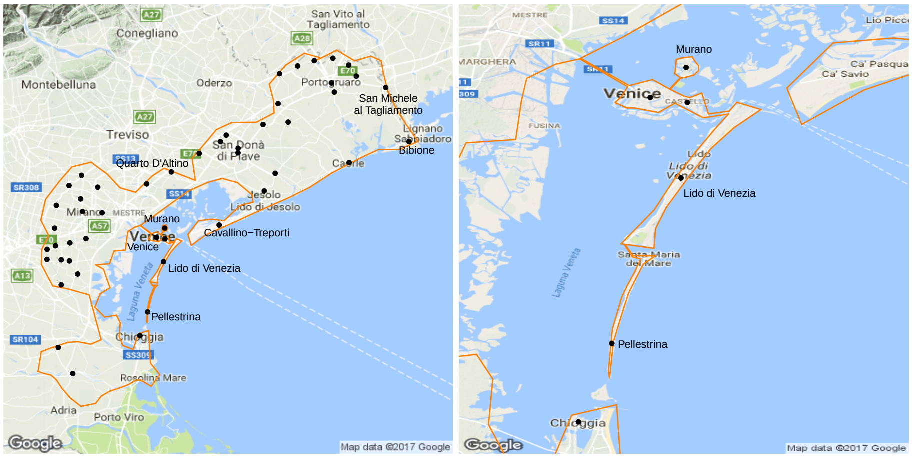

Figure 4: Simplified boundary of the Venice province. Figure adapted from [3].

and stationary. As detailed in the following paragraph, they induce the spatio-temporal mean and covariance structures of the estimator. Different regularizations may be considered, as briefly discussed in Paragraph 5, implying different mean and covariance structures and modelling anisotropic and non-stationary effects.

2.1 A separable spatio-temporal basis system

We represent the spatio-temporal field $f(\mathbf{p},t)$ as an expansion on a separable spatio-temporal basis system. Specifically, let $\{\varphi_k(t); k = 1,\ldots,M\}$ be a set of M basis functions defined on T and $\{\psi_l(\mathbf{p}); l = 1,\ldots,N\}$ a set of N basis functions defined on Ω. Then, f is represented by the following basis expansion:

$$f(\mathbf{p},t) = \sum_{l=1}^{N}\sum_{k=1}^{M} c_{lk}\ \psi_l(\mathbf{p})\ \varphi_k(t), \tag{3}$$

where $\{c_{lk}; l = 1,\ldots,N; k = 1,\ldots,M\}$ are the coefficients of the expansion on the separable spatio-temporal basis.

Various possible bases can be used for the expansions in the spatial and temporal domains. In this chapter, we describe the use, for the spatial domain, of a finite element basis on a triangulation Ω_τ of the domain Ω. This choice leads to an efficient discretization of the functional J and allows to accurately take into account the shape of the spatial domain.

We illustrate the construction of such basis on Venice domain. Before building the basis, we simplify the original spatial domain represented in Figure 1, excluding the coastal uninhabited regions and the smaller islands, and keeping in the domain of study only the four major islands: Venice, Murano (at the north-east of Venice), Lido di Venezia (at the south-east of Venice) and Pellestrina (at the south of Lido). We then smooth the boundary of the domain with regression splines. Finally, we obtain a piecewise linear boundary, sub-sampling from this smooth curve so that the features characterizing the domain are preserved. The left panel of Figure 4 shows the simplified boundary of Venice province, while the right panel of the same figure shows the detail around the city of Venice. This region is particularly interesting since it shows the four islands retained in the domain. Here the domain includes four bridges: one linking

Venice to the continent and the others linking some of the islands between themselves; the first one is an actual bridge with a road and a railway, while the other bridges represent regular and frequent ferries among the islands.

A triangulation of the resulting simplified domain is then obtained using the R package fdaPDE [14]. In particular, we start from a Delaunay triangulation, constrained within the simplified boundary, where each of the town locations and each point defining the simplified boundary become a triangle vertex. A more regular mesh is then obtained imposing a maximum value to the triangle areas. Figure 5 displays the resulting triangulation of Venice province. For this application, here and in Paragraph 4, instead of using as coordinates the latitude and longitude, we employ the UTM coordinate system, which allows to compute the distance between two points on the Earth's surface by means of the Euclidean distance instead of the geodesic distance.

Figure 5: Triangulation of the Venice province. Figure adapted from [3].

The finite element basis is composed by globally continuous functions that coincides with a polynomial of a certain degree on each element of the domain triangulation. In particular we use here linear finite element basis, that are piecewise linear functions. The dimension of the spatial basis is strictly related to the triangulation of the spatial domain: there is one basis function for each knot of the triangulation; for linear finite elements, each basis is associated to a vertex of the triangulation and has value 1 at that vertex and 0 at all other vertices. Figure 6 shows an example of linear basis function.

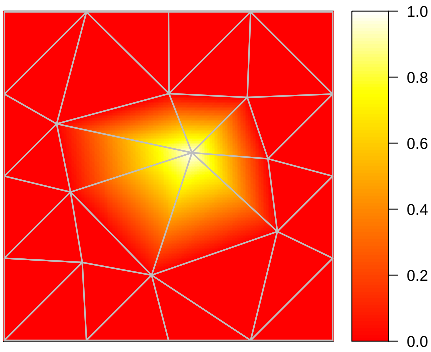

Figure 6: Example of linear finite element basis function.

For the temporal dimension, we use here a cubic B-spline basis with penalization of the second derivative, with knots coinciding with the sampling time instants of the dataset. Other basis systems may turn out to be more appropriate in other applicative contexts. For instance, Fourier basis are well suited to the case of cyclic data, possibly with penalization of the harmonic acceleration operator, instead of the order 2 derivative considered in (2).

The chosen basis system should be rich enough to enable an accurate representation of the spatio-temporal evolution of the phenomenon. In general, the number of bases, and thus of coefficients to be estimated, $M \times N$, can be larger than the sample size, $m \times n$. This is for instance the case of the application to Venice waste data, as well as of the simulation studies reported in Section 3. In these examples, in space we start from a contrained Delaunay triangulation of the spatial locations, that is further refined in the application to Venice waste data, and then consider the associated linear finite element basis, whose dimension N (equal to number of internal and boundary nodes) is thus larger than n. In time we use a cubic B-spline basis having knots at the m time instants of observation, resulting in a basis dimension M larger than m. This fact does not create any problem from the estimation point of view, thanks to the presence of the regularizing terms. We indeed never experienced any numerical instability of the method. Of course, in presence of dense sampling schemes, in space or time, coarser spatial or temporal grids may be preferred for computational saving.

2.2 Discretization of the penalized sum-of-square error functional

Let $\mathbf{z} \in \mathbb{R}^{nm}$ be the vector of observed data values at the $n \times m$ spatio-temporal locations, $\mathbf{f} \in \mathbb{R}^{nm}$ the vector of evaluations of the spatio-temporal function f at the $n \times m$ spatio-temporal locations, and $\mathbf{c} \in \mathbb{R}^{NM}$ the vector of coefficients of the basis expansion (3) of the spatio-temporal field f, with entries ordered as follows

$$\mathbf{z} = \begin{bmatrix} z_{11} \\ \vdots \\ z_{1m} \\ z_{21} \\ \vdots \\ z_{2m} \\ \vdots \\ z_{nm} \end{bmatrix} \qquad \mathbf{f} = \begin{bmatrix} f(\mathbf{p}_1, t_1) \\ \vdots \\ f(\mathbf{p}_1, t_m) \\ f(\mathbf{p}_2, t_1) \\ \vdots \\ f(\mathbf{p}_2, t_m) \\ \vdots \\ f(\mathbf{p}_n, t_m) \end{bmatrix} \qquad \mathbf{c} = \begin{bmatrix} c_{11} \\ \vdots \\ c_{1M} \\ c_{21} \\ \vdots \\ c_{2M} \\ \vdots \\ c_{NM} \end{bmatrix}.$$

Coherently, let $W \in \mathbb{R}^{nm \times q}$ be the design matrix containing the covariates $\{\mathbf{w}_{ij}; i = 1, ..., n; j = 1, ..., m\}$:

$$W = \begin{bmatrix} \mathbf{w}_{11}^T \\ \vdots \\ \mathbf{w}_{1m}^T \\ \mathbf{w}_{21}^T \\ \vdots \\ \mathbf{w}_{2m}^T \\ \vdots \\ \mathbf{w}_{nm}^T \end{bmatrix}.$$

Set $H_W = W(W^T W)^{-1} W^T$, the matrix that projects orthogonally into the subspace of $\mathbb{R}^{nm}$ generated by the columns of W, and set $Q = I_{nm} - H_W$, the matrix that projects into the orthogonal complement. We denote by $I_d \in \mathbb{R}^{d \times d}$ the identity matrix. Let $\Psi \in \mathbb{R}^{n \times N}$ be the matrix of the evaluations of the N spatial basis functions in the n spatial locations $\{\mathbf{p}_i; i = 1, ..., n\}$,

$$\Psi = \begin{bmatrix} \psi_1(\mathbf{p}_1) & \psi_2(\mathbf{p}_1) & \dots & \psi_N(\mathbf{p}_1) \\ \psi_1(\mathbf{p}_2) & \psi_2(\mathbf{p}_2) & \dots & \psi_N(\mathbf{p}_2) \\ \vdots & \vdots & \dots & \vdots \\ \psi_1(\mathbf{p}_n) & \psi_2(\mathbf{p}_n) & \dots & \psi_N(\mathbf{p}_n) \end{bmatrix}.$$

Moreover, define the vectors $\boldsymbol{\psi}, \boldsymbol{\psi}_x, \boldsymbol{\psi}_y \in \mathbb{R}^N$ of the spatial basis functions and of their first order partial derivatives:

$$\boldsymbol{\psi} = \begin{bmatrix} \psi_1 \\ \psi_2 \\ \vdots \\ \psi_N \end{bmatrix} \quad \boldsymbol{\psi}_x = \begin{bmatrix} \partial \psi_1 / \partial x \\ \partial \psi_2 / \partial x \\ \vdots \\ \partial \psi_N / \partial x \end{bmatrix} \quad \boldsymbol{\psi}_y = \begin{bmatrix} \partial \psi_1 / \partial y \\ \partial \psi_2 / \partial y \\ \vdots \\ \partial \psi_N / \partial y \end{bmatrix}.$$

Finally, let $R_0, R_1 \in \mathbb{R}^{N \times N}$ be two matrices respectively containing the integrals over Ω_τ of the cross products of the N spatial basis, and the integrals over Ω_τ of the cross products of the first derivatives of the N spatial basis, i.e.,

$$R_0 = \int_{\Omega_\tau} \boldsymbol{\psi} \boldsymbol{\psi}^T \qquad R_1 = \int_{\Omega_\tau} (\boldsymbol{\psi}_x \boldsymbol{\psi}_x^T + \boldsymbol{\psi}_y \boldsymbol{\psi}_y^T).$$

Analogously, let $\Phi \in \mathbb{R}^{m\times M}$ be the matrix of the evaluations of the M temporal basis functions in the m time instants $\{t_j; j = 1,...,m\}$:

$$\Phi = \begin{bmatrix} \varphi_1(t_1) & \varphi_2(t_1) & \dots & \varphi_M(t_1) \\ \varphi_1(t_2) & \varphi_2(t_2) & \dots & \varphi_M(t_2) \\ \vdots & \vdots & \dots & \vdots \\ \varphi_1(t_m) & \varphi_2(t_m) & \dots & \varphi_M(t_m) \end{bmatrix}.$$

Moreover, define the vectors $\boldsymbol{\varphi}, \boldsymbol{\varphi}_{tt} \in \mathbb{R}^M$ of the temporal basis functions and of their second order derivatives:

$$\boldsymbol{\varphi} = \begin{bmatrix} \varphi_1 \\ \varphi_2 \\ \vdots \\ \varphi_M \end{bmatrix} \quad \boldsymbol{\varphi}_{tt} = \begin{bmatrix} d^2\varphi_1/dt^2 \\ d^2\varphi_2/dt^2 \\ \vdots \\ d^2\varphi_M/dt^2 \end{bmatrix}.$$

Finally, let $K_0 \in \mathbb{R}^{M\times M}$ be the matrix of the integrals over T of the cross products of the M temporal basis, i.e.,

$$K_0 = \int_T \boldsymbol{\varphi}\boldsymbol{\varphi}^T . \tag{4}$$

Consider now the matrix $B = \Psi \otimes \Phi \in \mathbb{R}^{nm\times NM}$, where $\otimes$ denotes the Kronecker product. Then $\mathbf{f} = B\mathbf{c}$.

We may then rewrite the sum of square error functional J in (2) as

$$\begin{aligned} J &= (\mathbf{z} - W\boldsymbol{\beta} - B\mathbf{c})^T(\mathbf{z} - W\boldsymbol{\beta} - B\mathbf{c}) + \lambda_\Omega \mathbf{c}^T(P_S \otimes K_0)\mathbf{c} + \lambda_T \mathbf{c}^T(R_0 \otimes P_T)\mathbf{c} \\ &= (\mathbf{z} - W\boldsymbol{\beta} - B\mathbf{c})^T(\mathbf{z} - W\boldsymbol{\beta} - B\mathbf{c}) + \mathbf{c}^T P\mathbf{c}\ , \end{aligned} \tag{5}$$

where P_S and P_T are the matrix discretizations of the spatial and temporal penalization terms, and P is the overall penalty $P = \lambda_\Omega\ (P_S \otimes K_0)\ +\ \lambda_T\ (R_0 \otimes P_T)$. Specifically, the matrix P_T is obtained by direct discretization of the temporal penalty term in (2):

$$P_T = \int_T \boldsymbol{\varphi}_{tt}\boldsymbol{\varphi}_{tt}^T;$$

see [21] for details. For the matrix P_S, following [22] and [23], we consider a computationally efficient discretization of the spatial penalty term in (2), that does not involve the computation of second order derivatives of the basis functions, but only of first order derivatives. This discretization is given by $P_S = R_1 R_0^{-1} R_1$, and it is based on a variational characterization of the estimation problem; see [22] for details. As shown in [2], in the finite element space used to discretize the problem, the matrix P_S is in fact equivalent to the penalty matrix that would be obtained as direct discretization of the penalty term in (2) and involving the computation of second order derivatives.

This formulation uses the homogeneous Neumann condition at the boundary of the domain of interest implying zero flow across the boundary $\partial\Omega$. Boundary conditions are a way to control the behavior of the estimated function at the boundaries of the domain. Various boundary conditions are possible: Dirichlet conditions control the value of the function, that is $f|_{\partial\Omega} = \gamma_D$, Neumann conditions control the value of the normal derivative of the function, that is $\partial_{\mathbf{n}} f|_{\partial\Omega} = \gamma_N$, and Robin conditions are linear combinations of the previous two. Homogeneous conditions correspond to the case when γ_D or γ_N are null functions. Moreover, different types of boundary conditions can be imposed on different parts of the boundary, forming a partition of it. In the simulations reported in Section 3 and in the application to Venice waste data, we impose homogeneous Neumann boundary conditions, i.e., null flow across the boundary; we are thus considering closed systems with respect to the phenomenon considered. In the context of Venice data, this means that we assume no exchange of waste between Venice province and the sea, or between Venice province and other neighboring provinces.

To compute the estimates of the vector of regression coefficients $\boldsymbol{\beta}$ and of the vector $\mathbf{c}$ of coefficients of the basis expansion of the spatio-temporal field f, we compute the first partial derivatives of J with respect to $\boldsymbol{\beta}$ and $\mathbf{c}$, and set them equal to zero, getting the following explicit solution to the estimation problem:

$$\begin{aligned}\hat{\boldsymbol{\beta}} &= (W^T W)^{-1} W^T (\mathbf{z} - B\hat{\mathbf{c}}),\\ \hat{\mathbf{c}} &= (B^T Q B + P)^{-1} B^T Q \mathbf{z}.\end{aligned}$$

The estimators are linear in the observed data values $\mathbf{z}$; the estimator $\hat{\mathbf{c}}$ has a penalized least-square form and, given $\hat{\mathbf{c}}$, the estimator $\hat{\boldsymbol{\beta}}$ has a least-square form.

2.3 Properties of the estimators

Let $S_{\mathbf{f}} = B(B^T Q B + P)^{-1} B^T Q$, so that $\hat{\boldsymbol{\beta}} = (W^T W)^{-1} W^T (I_{nm} - S_{\mathbf{f}})\mathbf{z}$.

Since $E[\mathbf{z}] = W\boldsymbol{\beta} + \mathbf{f}$ and $Var[\mathbf{z}] = \sigma^2 I_{nm}$, and exploiting the fact that the matrix Q is idempotent and $QW = 0$ (where 0 is the $nm \times q$ zero matrix), we obtain

$$\begin{aligned}E[\hat{\mathbf{c}}] &= (B^T Q B + P)^{-1} B^T Q \mathbf{f},\\ Var[\hat{\mathbf{c}}] &= \sigma^2 (B^T Q B + P)^{-1} B^T Q B (B^T Q B + P)^{-1}\end{aligned}$$

and

$$\begin{aligned}E[\hat{\boldsymbol{\beta}}] &= \boldsymbol{\beta} + (W^T W)^{-1} W^T (I_{nm} - S_{\mathbf{f}})\mathbf{f},\\ Var[\hat{\boldsymbol{\beta}}] &= \sigma^2 (W^T W)^{-1} + \sigma^2 (W^T W)^{-1} W^T S_{\mathbf{f}} S_{\mathbf{f}}^T W (W^T W)^{-1}.\end{aligned} \tag{6}$$

Consider the vector $\mathbf{B}(\mathbf{p},t) = \boldsymbol{\psi}(\mathbf{p})^T \otimes \boldsymbol{\varphi}(t)^T$ of evaluations of the separable basis system at the spatio-temporal location $(\mathbf{p},t) \in \Omega \times T$. The estimate of the field f at this generic location is thus given by

$$\hat{f}(\mathbf{p},t) = \mathbf{B}(\mathbf{p},t)\hat{\mathbf{c}} = \mathbf{B}(\mathbf{p},t)(B^T Q B + P)^{-1} B^T Q \mathbf{z}$$

and its mean and variance are given by

$$\begin{aligned}E[\hat{f}(\mathbf{p},t)] &= \mathbf{B}(\mathbf{p},t)(B^T Q B + P)^{-1} B^T Q \mathbf{f}\\ Var[\hat{f}(\mathbf{p},t)] &= \sigma^2 \mathbf{B}(\mathbf{p},t)(B^T Q B + P)^{-1} B^T Q B (B^T Q B + P)^{-1} \mathbf{B}(\mathbf{p},t)^T,\end{aligned} \tag{7}$$

with covariance at any two spatio-temporal locations $(\mathbf{p}_1,t_1),(\mathbf{p}_2,t_2) \in \Omega \times T$ given by

$$\begin{aligned}&Cov[\hat{f}(\mathbf{p}_1,t_1),\hat{f}(\mathbf{p}_2,t_2)] =\\ &\qquad \sigma^2 \mathbf{B}(\mathbf{p}_1,t_1)(B^T Q B + P)^{-1} B^T Q B (B^T Q B + P)^{-1} \mathbf{B}(\mathbf{p}_2,t_2)^T.\end{aligned} \tag{8}$$

It should be noticed that the regularizing terms in (2), and their corresponding discretization P, induce both the first order structure (i.e., the mean) and the second order structure (i.e., the spatio-temporal covariance) of the estimator $\hat{f}$. Different regularizations would imply different mean and covariance structures. For instance, [2] consider a regularized spatial regression model and show that by changing the regularizing term and considering more complex differential operators it is possible to include in the model a priori information about the spatial variation of the phenomenon, and to model also anisotropies and non-stationarities.

The smoothing matrix S, which maps the vector of observed values $\mathbf{z}$ to the vector of fitted values $\hat{\mathbf{z}} = S\mathbf{z}$, is given by

$$S = H_W + QS_{\mathbf{f}}.$$

The trace of the smoothing matrix constitutes a commonly used measure of the equivalent degrees of freedom for linear estimators (this notion was first introduced by [4]). For the model considered, this is given by $\mathrm{tr}(S) = q + \mathrm{tr}(S_{\mathbf{f}})$, thus coinciding with the sum of the q degrees of freedom corresponding to the parametric part of the model and the $\mathrm{tr}(S_{\mathbf{f}})$ degrees of freedom corresponding to the non-parametric part of the model. A robust estimator of σ^2 is given by

$$\hat{\sigma}^2 = \frac{1}{nm - \mathrm{tr}(S)} (\mathbf{z} - \hat{\mathbf{z}})^T (\mathbf{z} - \hat{\mathbf{z}}). \tag{9}$$

This estimate of the error variance, plugged into (7), can be used to compute approximate Gaussian pointwise confidence intervals for f; similarly, plugged into (6), it can be used to compute approximate Gaussian confidence intervals for $\boldsymbol{\beta}$. Moreover, the value of a new observation at the spatial location $\mathbf{p}_{n+1} \in \Omega$ and time instant $t_{m+1} \in T$, and with associated covariates $\mathbf{w}_{n+1\ m+1}$, can be predicted by $\hat{z}_{n+1\ m+1} = \mathbf{w}_{n+1\ m+1}^T\ \hat{\boldsymbol{\beta}}\ + \hat{f}(\mathbf{p}_{n+1}, t_{m+1})$, and approximate prediction intervals may as well be constructed.

Finally, the values of the smoothing parameters λ_Ω and λ_T may be chosen via Generalized Cross-Validation (GCV), searching for the values of λ_Ω and λ_T that minimize

$$GCV(\lambda_\Omega, \lambda_T) = \frac{nm}{(nm - \mathrm{tr}(S))^2} (\mathbf{z} - \hat{\mathbf{z}})^T (\mathbf{z} - \hat{\mathbf{z}}).$$

2.4 Model without covariates

If covariates are not included in the model, than (1) is replaced by

$$z_{ij} = f(\mathbf{p}_i, t_j)\ +\ \varepsilon_{ij} \quad i = 1, ..., n,\ \ j = 1, ..., m,$$

a classical functional data analysis model. The spatio-temporal field f can thus be estimated minimizing the functional

$$\begin{aligned} J(f) \quad &= \quad \sum_{i=1}^{n} \sum_{j=1}^{m} \big(z_{ij} - f(\mathbf{p}_i, t_j)\big)^2\ + \\ &\quad +\lambda_\Omega \int_T \int_\Omega \Big(\Delta f(\mathbf{p}, t)\Big)^2 d\mathbf{p} dt + \lambda_T \int_\Omega \int_T \Big(\frac{\partial^2 f(\mathbf{p}, t)}{\partial t^2}\Big)^2 dt d\mathbf{p}. \end{aligned} \tag{10}$$

The numerical discretization of the functional follows as in Section 2.1, leading to

$$J = (\mathbf{z} - B\mathbf{c})^T (\mathbf{z} - B\mathbf{c}) + \mathbf{c}^T P \mathbf{c}\ ,$$

and hence to the following estimator of the vector of coefficients for the spatio-temporal field:

$$\hat{\mathbf{c}} \quad = \quad (B^T B + P)^{-1} B^T \mathbf{z}.$$

The mean and variance of this estimator are given by

$$\begin{aligned} E[\hat{\mathbf{c}}] &= (B^T B + P)^{-1} B^T \mathbf{f}, \\ Var[\hat{\mathbf{c}}] &= \sigma^2 (B^T B + P)^{-1} B^T B (B^T B + P)^{-1}. \end{aligned}$$

The estimator of the field f at a generic location $(\mathbf{p}, t)$ is thus given by

$$\hat{f}(\mathbf{p}, t) = \mathbf{B}(\mathbf{p}, t)\hat{\mathbf{c}} = \mathbf{B}(\mathbf{p}, t)(B^T B + P)^{-1} B^T \mathbf{z}$$

and has the following mean, variance and covariance structures

$$\begin{aligned} E[\hat{f}(\mathbf{p}, t)] &= \mathbf{B}(\mathbf{p}, t)(B^T B + P)^{-1} B^T \mathbf{f} \\ Var[\hat{f}(\mathbf{p}, t)] &= \sigma^2 \mathbf{B}(\mathbf{p}, t)(B^T B + P)^{-1} B^T B (B^T B + P)^{-1} \mathbf{B}(\mathbf{p}, t)^T \\ Cov[\hat{f}(\mathbf{p}_1, t_1), \hat{f}(\mathbf{p}_2, t_2)] &= \sigma^2 \mathbf{B}(\mathbf{p}_1, t_1)(B^T B + P)^{-1} B^T B (B^T B + P)^{-1} \mathbf{B}(\mathbf{p}_2, t_2)^T. \end{aligned}$$

These above expressions coincide with those derived in Paragraph 2.3, setting $Q = I$. As noted earlier, the mean and covariance structure of the estimator are characterized by the chosen regularizing terms, through their discretization P. Finally, the smoothing matrix is in this case given by $S = B(B^T B + P)^{-1} B^T$. The computation of the degrees of freedom of the estimator, the estimate of the error variance, the optimal selection of the smoothing parameters λ_Ω and λ_T, and the computation of confidence/prediction intervals follows along the same lines outlined in the case of the model with covariates.

2.5 An alternative formulation of the model

Instead of considering the functionals (2) or (10), respectively in the case with or without covariates, it is possible to consider alternative functionals, that regularize directly the coefficients of the basis expansion of the spatio-temporal field, in analogy with the models proposed by [1] and [15]. This alternative formulation is detailed in [3], Section 5.

3 Simulation studies

In [3] the performances of the proposed spatio-temporal regression with PDE regularization (ST-PDE) are tested via extensive simulation studies under various settings, with different sampling designs in space and time, with and without covariates, with correlated and uncorrelated noise. Spatial regression with differential regularization is compared to separable spatio-temporal kriging, to the space-time models proposed by [1] and [15] and based on soap film smoothing [26], and to an analogous space-time model based on thin-plate splines. We here report the results from two simulation studies, referring the interested reader to [3] for details.

We consider a test function defined on a C-shaped spatial domain, shown at three different time instants in the first row of Figure 7. The test function displays similar features as Venice waste data: its domain is characterized by a strong concavity, and different values of the field are observed in the two arms of the domain, across the concavity, with different behaviors over time. The second row in Figure 7 shows the data sampled at the three time instants, for the first simulation replicate.

The implementation of ST-PDE is based on the R package fdaPDE [14]. In space we use a linear finite element basis defined on the mesh shown in the second row of Figure 7, a contrained Delaunay triangulation of the sampling spatial locations. In time we use a cubic B-spline basis, with knots coinciding with the sampling time instants. The values of the smoothing parameters λ_Ω and λ_T are chosen via GCV. The field estimate obtained in the first simulation replicate, at the three considered time instants, is shown in the last row of Figure 7. The third and fourth rows of the same figure illustrate instead the field estimates obtained by spatio-temporal kriging (KRIG), implemented using the R package gstat [19], and by spatio-temporal smoothing with a thin-plate spline basis in space and a B-spline basis in time (TPS), implemented using the R package mgcv [25]. For the kriging we use a separable variogram marginally Gaussian in space and exponential in time, with parameters estimated from the empirical variogram. For the spatio-temporal model based on thin-plate splines we select the smoothing parameters via GCV. Figure 7 shows that KRIG and TPS return poor estimates of the true spatio-temporal field, especially in those time instants where the true field is characterized by different values in the two arms of the C-shaped domain (see the first and second columns in the figure): the different values have in fact been smoothed across the concavity in the domain. ST-PDE instead accurately estimates the spatio-temporal field, being able to comply with the shape of the domain. The left panel of Figure 9 shows the boxplots of the Root Mean Square Errors (RMSE), over 50 replicates of the noise generation, of the space-time field estimates yielded by the three methods. These boxplots confirm the comparative advantage of ST-PDE over KRIG and TPS.

Figure 8 and the right panel of Figure 9 show the results from a second simulation study detailed in [3], where we as well include a space-time varying covariate. The second row in Figure 8 shows the added contributions of covariates and true function. In this simulation setting we do not compare to spatio-temporal kriging, as the function `krigeST` of the R package gstat does not allow for the inclusion of covariates. The results are otherwise similar to those obtained in the simulation without covariates, with a superiority of ST-PDE over TPS. This superiority also reflects in the estimation of the β coefficient: the corresponding RMSE over the 50 replicates is 0.14 for TPS and 0.09 for ST-PDE. Also in this simulation setting, the main reason of the comparative advantage shown by ST-PDE consists in its ability to comply with the shape of the domain.

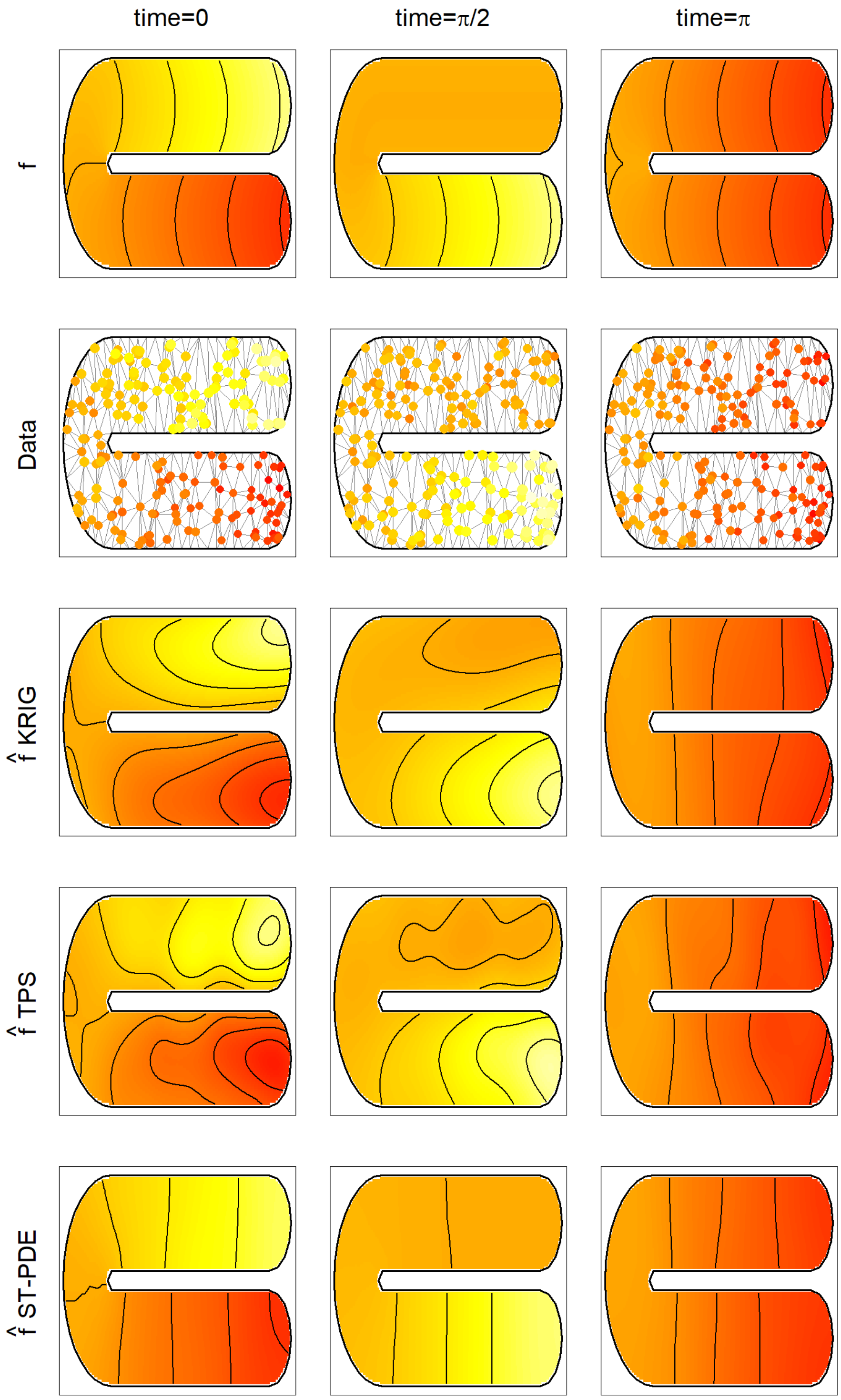

Figure 7: Simulation without covariates: test function (first row), sampled data (second row), field estimates provided by spatio-temporal kriging (third row), by spatio-temporal smoothing using thin-plate splines (fourth row) and by ST-PDE (fifth row).

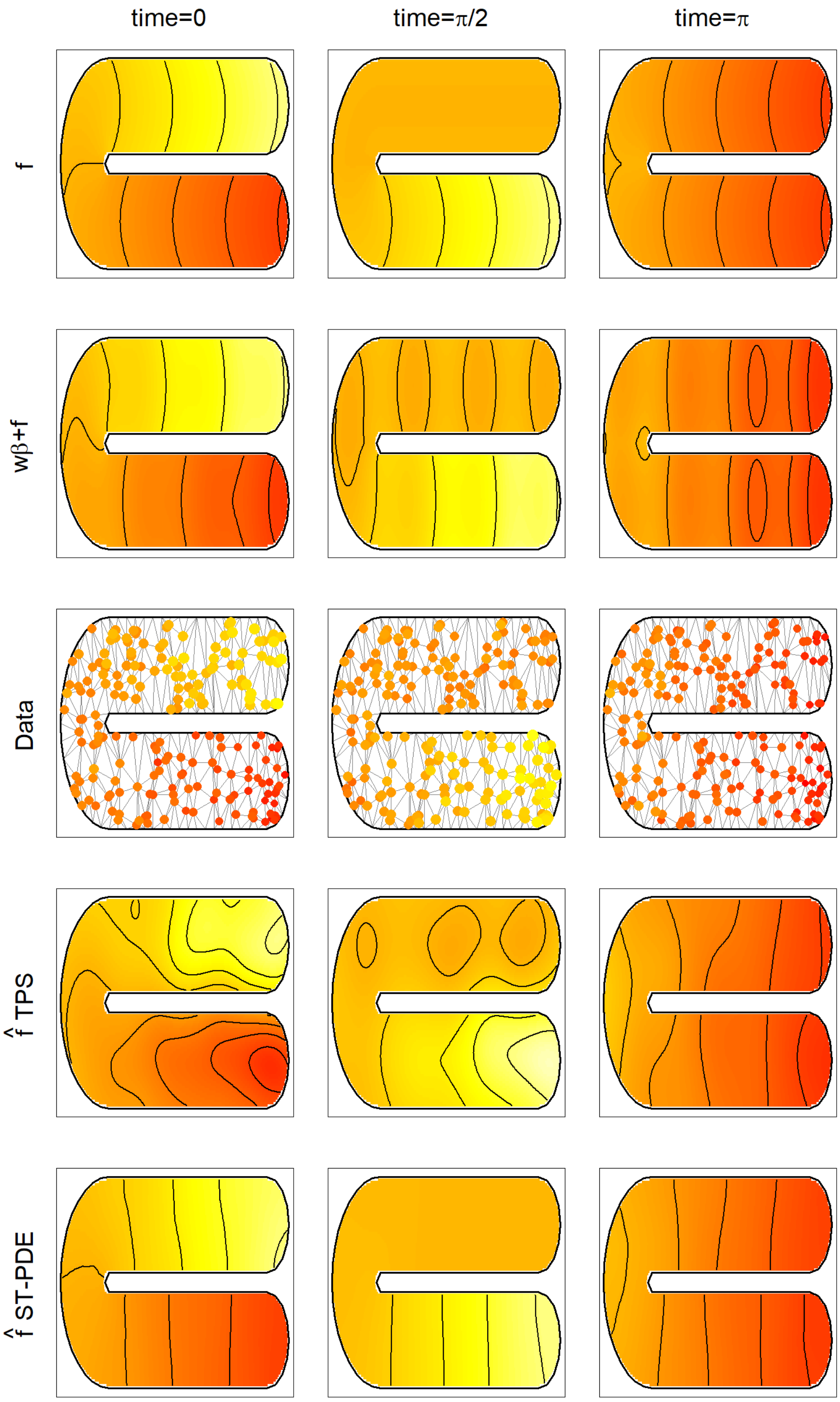

Figure 8: Simulation with covariates: test function (first row), added contributions of the spatio-temporal covariate field and of the test function (second row), sampled data (third row), field estimates provided by spatio-temporal smoothing using thin-plate splines (fourth row) and by ST-PDE (fifth row).

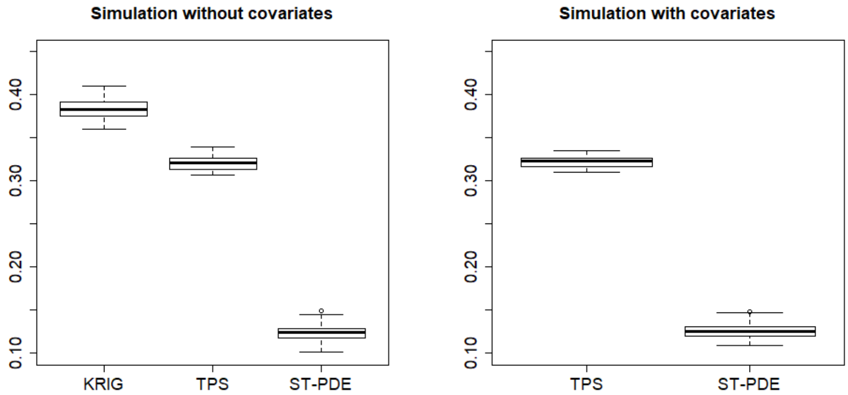

Figure 9: Left. Simulation without covariates: boxplots of the RMSE, over 50 simulation replicates, of the field estimates provided by spatio-temporal kriging (KRIG), by spatio-temporal smoothing using thin-plate splines (TPS) and by spatio-temporal regression with PDE regularization (ST-PDE). Right. Simulation with covariates: boxplots of the RMSE, over 50 simulation replicates, of the field estimates provided by spatio-temporal smoothing using thin-plate splines (TPS) and by spatio-temporal regression with PDE regularization (ST-PDE).

4 An illustrative example: study of the waste production in Venice province

We now illustrate the described method via an application to the study of the annual amount of per capita municipal waste produced in the Venice province.

4.1 The Venice waste dataset

Open Data Veneto[1] provides the gross and per capita annual amount of municipal waste produced in each municipality of the Venice province in the period from 1997 to 2011. We here consider for the analysis the annual per capita municipal waste, in kg per municipality resident.

Municipal waste includes that produced in houses and public areas, but does not include special waste, i.e. industrial, agricultural, construction and demolition waste, or hazardous waste, for which there are special disposal programs. Therefore, the data refer only to the urbanized areas of the municipality, whilst they do not refer to the agricultural or industrial areas in the municipality territories. Since no data identifying the urbanized areas of the municipalities is available, we face here two possible simplifications of the problem. We can either partition the Venice province in the municipality territories and attribute each datum to the whole territory of its municipality, or assign each datum to a point representing the center of the municipality. We here adopt the second simplification. The spatial coordinates of the town centers are available online[2]. As mentioned in Paragraph 2.1, latitude and longitude are converted into UTM coordinate system.

[1] http://dati.veneto.it/dataset/produzione-annua-di-rifiuti-urbani-totale-e-pro-capite-1997-2011
[2] http://www.dossier.net/utilities/coordinate-geografiche/

In some cases there are localities which do not constitute a municipality on their own, but are under the jurisdiction of another town. In this case, there are two or more main urbanized areas in the municipality territory. Some of these localities are not negligible for the problem under analysis due to their tourist relevance and their location on the domain; for this reason we add them to the data. Specifically, we include the seaside town of Bibione, the easternmost village indicated in Figure 1. This popular vacation destination falls under the jurisdiction of the municipality of San Michele al Tagliamento, north west of Bibione; the waste data considered for Bibione are a replicate of the data of San Michele al Tagliamento. Moreover, we replicate the data of Venice in the islands of Murano, Lido di Venezia and Pellestrina, because of their tourist relevance and the particular shape of the domain.

We include as a covariate the number of beds in accommodation facilities (such as hotels, bed and breakfast, guest houses, campings, etc.) divided by the number of residents. This ratio may be as large as 7 in some tourist towns by the sea. The number of beds in accommodation facilities is provided by Istat[3], the Italian national institute for statistics.

4.2 Analysis of Venice waste data by spatial regression with differential regularization

Figure 10 shows the estimated spatio-temporal field at fixed time instants. The estimate for the coefficient β is 39.7 meaning that one more unit in the ratio between the number of beds in accommodation facilities and the number of residents is estimated to increase the yearly per capita production of waste by residents by about 40kg. The estimated spatial field f shows the highest values, across the years, in correspondence of the coastline, around the towns of Bibione, Lido di Jesolo and Cavallino-Treporti. These higher values may be due to a type of tourism that is not captured by the available covariate, such as daily tourists who do not stay overnight, and vacationers who either own or rent vacation houses. The higher values of the field are also probably due to the presence of many seasonal workers, who are not residents of these towns, and are employed in the numerous accommodation facilities, restaurants, cafés, shops, beach resorts and other services.

Although Venice is one of the most visited cities in Italy, and this tourism is active all year round, the production of per capita waste in Venice appears to be lower than in other nearby tourist localities by the seaside. This might be partly explained by the fact that the tourist activities in Venice are not so highly characterized by seasonality as in the smaller seaside villages, and people working in tourist activities in Venice are more likely to be themselves residents of this large city.

It is significant to notice how the estimated function does not smooth across concave boundaries. For example, the area of the city of Quarto d'Altino and the one around the city of Cavallino-Treporti show different ranges of values. Indeed, even though the two towns are geographically close, they are separated by the Venetian lagoon. This difference is evident also from the first two panels of Figure 11, which shows the estimated spatio-temporal field at fixed localities: Quarto d'Altino, Cavallino-Treporti, Venice and Bibione. In these plots the dots are obtained subtracting from the data the estimated contribution by the covariate, i.e. $\hat{\beta} w_{ij}$.

The temporal evolution plots in Figure 11 show the ability of the method to capture the temporal trend of the phenomenon. The method provides good estimates also for the municipality of Cavallino-Treporti, which presents a strong variation of per capita

[3]http://www.istat.it/it/archivio/113712

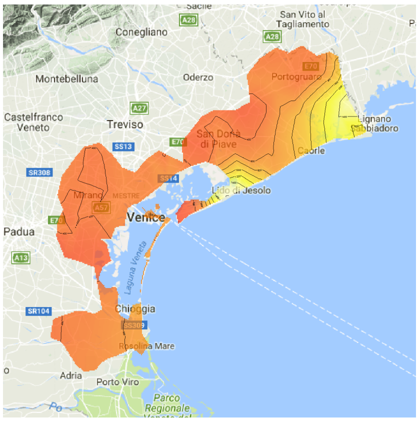

(a) 1997

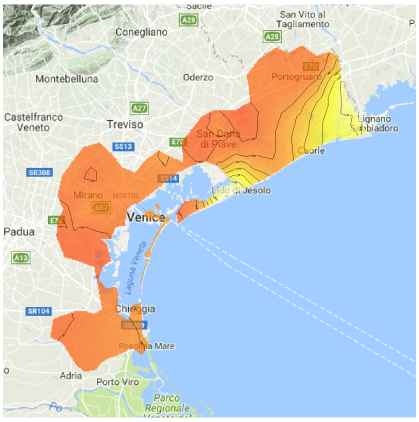

(b) 2000

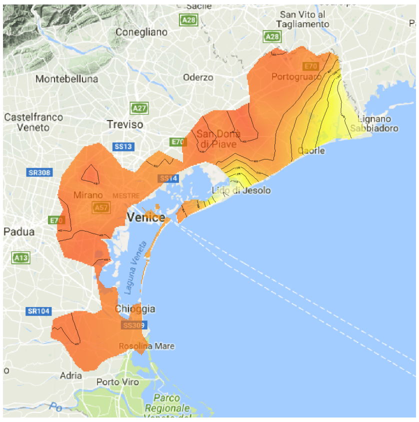

(c) 2003

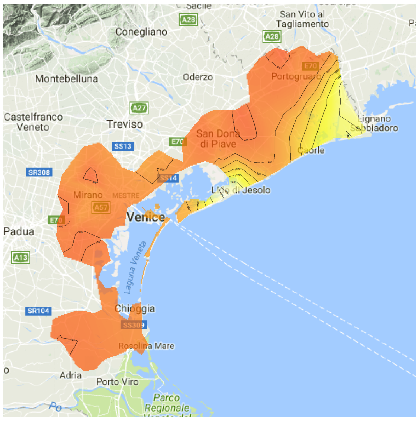

(d) 2006

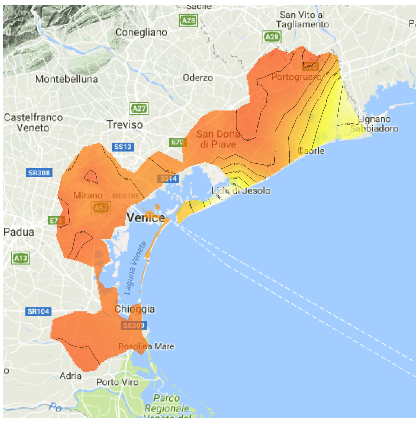

(e) 2009

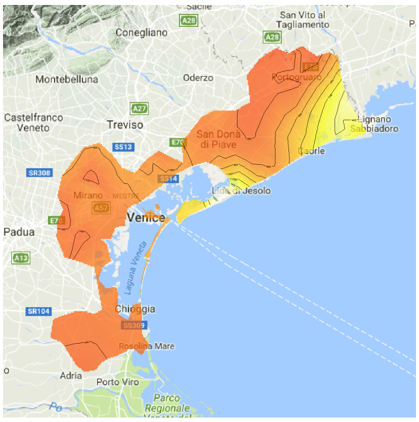

(f) 2011

Figure 10: Estimated spatio-temporal field for the Venice waste data (yearly per capita production) at fixed time instants.

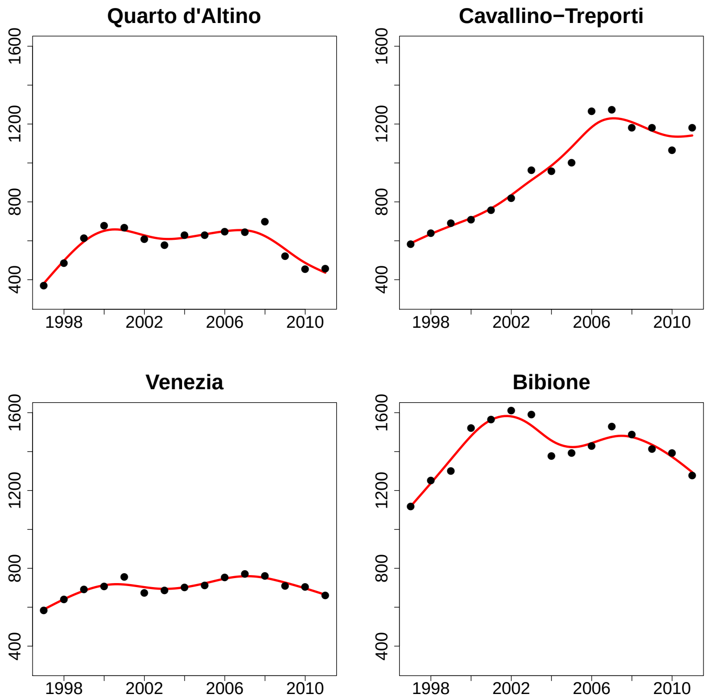

Figure 11: Temporal evolution of the estimated spatio-temporal field for the Venice waste data (yearly per capita production) at fixed spatial locations. Figure adapted from [3].

waste over the year. The large increase of the per capita waste of Cavallino-Treporti is partly explained by the fact that, during the first years of this study, this town was under the jurisdiction of Venice, while the data for this new municipality are available only from 2002. In particular, the data for Cavallino-Treporti for years 1997 to 2001 are a replicate of the data of the municipality of Venice. Nevertheless, the strong variation in the data is well captured by the estimated function.

5 Model extensions

Various extensions of the model described in this chapter are possible. A first generalization consists in modelling data that are areal in space and integral in time, and estimating an underlying spatio-temporal intensity function. In the application to Venice waste data, if information about the urbanized areas of each municipality would become available, such a model extension would for instance allow to appropriately refer the waste datum to the area and year where it is produced, estimating a spatio-temporal intensity of waste production.

Extending the work of [2] it is also possible to include a priori information available on the phenomenon under study, using more complex differential regularizations modelling the spatial and/or temporal behavior of the phenomenon. This also allows to account for non-stationarities and anisotropies in space and/or time. Along the same lines, if a priori information about the interaction between space and time was available, then it would make sense to consider a unique space/time regularizing term based on a time-dependent PDE that governs the phenomenon behavior. [2] for instance analyze the blood flow velocity in a section of the carotid artery at a fixed time instant corresponding to the systolic peak, starting from Echo-Color Doppler data, and including a priori information on the problem under study. By introducing the time dimension, we could study how the blood flow velocity field varies during the time of the heart-beat. PDEs are commonly used to describe complex phenomena behavior in many fields of engineering and sciences, including bio-sciences, geo-sciences, and physical sciences. Potential applications of particular interest of this space-time technique in the environmental sciences would for example concern the study of the dispersion of pollutant released in water or in air and transported by streams or winds, and the study of the propagation of earthquakes, tsunamis, and other wave phenomena. If one wishes instead to consider simpler isotropic and stationary regularizations, then a possibility to allow for stronger interactions in space/time, with respect to the model here presented, would consists in defining a unique regularizing term based on a heat equation.

Finally, data distributed over curved domains, instead of over planar domains, could be handled by extending the model proposed in [9]. Considering the same application presented by [9], this would for instance enable the study of time-dependent hemodynamic forces exerted by blood-flow over the wall of inner carotid arteries affected by aneurysms, taking into account the complex morphology of these vessels. Another fascinating field of application of this modelling extension would be in the neurosciences [7][13], studying signals associated to neuronal activity over the cortical surface, a highly convoluted thin sheet of neural tissue that constitutes the outermost part of the brain. In the geo-sciences, this would permit the study of data distributed over regions with complex orographies. Moreover, generalizations to time-dependent data of the spatial regression model introduced by [24] would be particularly well suited for important engineering applications, especially in the automotive, naval, aircraft and space sectors, where space-time varying quantities of interest are observed over the surface of a designed 3D object, such as the pressure over the surface of a shuttle winglet.

References

[1] Nicole H Augustin, Verena M Trenkel, Simon N Wood, and Pascal Lorance. Space-time modelling of blue ling for fisheries stock management. *Environmetrics*, 24(2):109–119, 2013.

[2] Laura Azzimonti, Laura M Sangalli, Piercesare Secchi, Maurizio Domanin, and Fabio Nobile. Blood flow velocity field estimation via spatial regression with PDE penalization. *Journal of the American Statistical Association*, 110(511):1057–1071, 2015.

[3] Mara S Bernardi, Laura M Sangalli, Gabriele Mazza, and James O Ramsay. A penalized regression model for spatial functional data with application to the analysis of the production of waste in venice province. *Stochastic Environmental Research and Risk Assessment*, 31(1):23–38, 2017.

[4] Andreas Buja, Trevor Hastie, and Robert Tibshirani. Linear smoothers and additive models. *The Annals of Statistics*, pages 453–510, 1989.

[5] William Caballero, Ramón Giraldo, and Jorge Mateu. A universal kriging approach for spatial functional data. *Stochastic Environmental Research and Risk Assessment*, 27(7):1553–1563, 2013.

[6] Noel Cressie and Christopher K Wikle. *Statistics for spatio-temporal data*. John Wiley & Sons, 2011.

[7] Franco Dassi, Bree Ettinger, Simona Perotto, and Laura M Sangalli. A mesh simplification strategy for a spatial regression analysis over the cortical surface of the brain. *Applied Numerical Mathematics*, 90:111–131, 2015.

[8] Pedro Delicado, Ramón Giraldo, C Comas, and Jorge Mateu. Statistics for spatial functional data: some recent contributions. *Environmetrics*, 21(3-4):224–239, 2010.

[9] Bree Ettinger, Simona Perotto, and Laura M Sangalli. Spatial regression models over two-dimensional manifolds. *Biometrika*, 103(1):71–88, 2016.

[10] R Giraldo, P Delicado, and J Mateu. Ordinary kriging for function-valued spatial data. *Environmental and Ecological Statistics*, 18(3):411–426, 2011.

[11] M Goulard and M Voltz. Geostatistical interpolation of curves: A case study in soil science. In *Geostatistics Tróia'92*, pages 805–816. Springer, 1993.

[12] Rosaria Ignaccolo, Jorge Mateu, and Ramon Giraldo. Kriging with external drift for functional data for air quality monitoring. *Stochastic Environmental Research and Risk Assessment*, 28(5):1171–1186, 2014.

[13] Eardi Lila, John AD Aston, and Laura M Sangalli. Smooth principal component analysis over two-dimensional manifolds with an application to neuroimaging. *The Annals of Applied Statistics*, 10(4):1854–1879, 2016.

[14] Eardi Lila, Laura M. Sangalli, Jim Ramsay, and Luca Formaggia. *fdaPDE: Regression with Partial Differential Regularizations, using the Finite Element Method*, 2016. R package version 0.1-1.

[15] Giampiero Marra, David L Miller, and Luca Zanin. Modelling the spatiotemporal distribution of the incidence of resident foreign population. *Statistica Neerlandica*, 66(2):133–160, 2012.

[16] Alessandra Menafoglio, Piercesare Secchi, and Matilde Dalla Rosa. A Universal Kriging predictor for spatially dependent functional data of a Hilbert Space. *Electronic Journal of Statistics*, 7:2209–2240, 2013.

[17] Alessandra Menafoglio, Alberto Guadagnini, and Piercesare Secchi. A kriging approach based on Aitchison geometry for the characterization of particle-size curves in heterogeneous aquifers. *Stochastic Environmental Research and Risk Assessment*, 28(7):1835–1851, 2014.

[18] David Nerini, Pascal Monestiez, and Claude Manté. Cokriging for spatial functional data. *Journal of Multivariate Analysis*, 101(2):409–418, 2010.

[19] Edzer J. Pebesma. Multivariable geostatistics in S: the gstat package. *Computers & Geosciences*, 30:683–691, 2004.

[20] R Core Team. *R: A Language and Environment for Statistical Computing*. R Foundation for Statistical Computing, Vienna, Austria, 2014.

[21] James O Ramsay and Bernard W Silverman. *Functional Data Analysis*. Springer, 2005.

[22] Tim Ramsay. Spline smoothing over difficult regions. *Journal of the Royal Statistical Society: Series B (Statistical Methodology)*, 64(2):307–319, 2002.

[23] Laura M Sangalli, James O Ramsay, and Timothy O Ramsay. Spatial spline regression models. *Journal of the Royal Statistical Society: Series B (Statistical Methodology)*, 75(4):681–703, 2013.

[24] Matthieu Wilhelm, Luca Dedè, Laura M Sangalli, and Pierre Wilhelm. IGS: an IsoGeometric approach for Smoothing on surfaces. *Computer Methods in Applied Mechanics and Engineering*, 2016.

[25] Simon Wood. *Generalized additive models: an introduction with R*. CRC press, 2006.

[26] Simon N Wood, Mark V Bravington, and Sharon L Hedley. Soap film smoothing. *Journal of the Royal Statistical Society: Series B (Statistical Methodology)*, 70(5):931–955, 2008.

MOX Technical Reports, last issues

Dipartimento di Matematica
Politecnico di Milano, Via Bonardi 9 - 20133 Milano (Italy)

43/2018 Fontana, L.; Masci, C.; Ieva, F.; Paganoni, A.M.
Performing Learning Analytics via Generalized Mixed-Effects Trees

42/2018 Antonietti, P.F.; Melas, L.
Algebraic multigrid schemes for high-order discontinuous Galerkin methods

41/2018 Mazzieri, I.; Melas, L.; Smerzini, C.; Stupazzini, M.
The role of near-field ground motion on seismic risk assessment in large urban areas

40/2018 Chiappa, A.S.; Micheletti, S.; Peli, R.; Perotto, S.
Mesh adaptation-aided image segmentation

38/2018 Domanin, M.; Gallo, D.; Vergara, C.; Biondetti, P.; Forzenigo, L.V.; Morbiducci, U.
Prediction of long term restenosis risk after surgery in the carotid bifurcation by hemodynamic and geometric analysis

39/2018 Ferro, N.; Micheletti, S.; Perotto, S.
Density-based inverse homogenization with anisotropically adapted elements

37/2018 Bonaventura, L.; Della Rocca A.;
Convergence analysis of a cell centered finite volume diffusion operator on non-orthogonal polyhedral meshes

35/2018 Possenti, L.; Casagrande, G.; Di Gregorio, S.; Zunino, P.; Costantino, M.L.
Numerical simulations of the microvascular fluid balance with a non-linear model of the lymphatic system

34/2018 Laurino, F.; Coclite, A.; Tiozzo, A.; Decuzzi, P.; Zunino, P.;
A muliscale computational approach for the interaction of functionalized nanoparticles with the miscrovasculature

32/2018 Dal Santo, N.; Deparis, S.; Manzoni, A.; Quarteroni, A.
An algebraic least squares reduced basis method for the solution of nonaffinely parametrized Stokes equations